Continuous-flow synthesis and application of polymer-supported BODIPY Photosensitisers for the generation of singlet oxygen; process optimised by in-line NMR spectroscopy

Journal of Flow Chemistry
https://doi.org/10.1007/s41981-019-00067-4

FULL PAPER

Continuous-flow synthesis and application of polymer-supported BODIPY Photosensitisers for the generation of singlet oxygen; process optimised by in-line NMR spectroscopy

Christopher G. Thomson[1] · Callum M. S. Jones[2] · Georgina Rosair[1] · David Ellis[1] · Jose Marques-Hueso[2] · Ai-Lan Lee[1] · Filipe Vilela[1]

Received: 29 October 2019 / Accepted: 27 November 2019

Abstract

Commercial polystyrene Merrifield-type resins have been post-synthetically functionalised with BODIPY photosensitisers via a novel aryl ester linking strategy in continuous-flow. A unique synthetic advantage of post-synthetically modifying heterogeneous materials in flow was identified. The homogeneous analogues of the polymer-supported BODIPYs were synthesised and used as reference to assess photophysical properties altered by the polymer-support and linker. The homogeneous and polymer-supported BODIPYs were applied in visible-light photosensitisation of singlet oxygen for the conversion of α-terpinene to ascaridole. Materials produced in flow were superior to batch in terms of functional loading and photosensitisation efficiency. Flow photochemical reactions generally outperformed batch by a factor of 4 with respect to rate of reaction. The polymer-supported BODIPY resins could be irradiated for 96 h without loss of photosensitising ability. Additional material synthetic modification and conditions optimisation using an in-line NMR spectrometer resulted in a 24-fold rate enhancement from the initial material and conditions.

Keywords BODIPY · In-line NMR reaction monitoring · Merrifield resins · Organic photosensitisers · Singlet oxygen · Visible light

Introduction

Development of organic photocatalysts and photosensitisers has had significant interest in the past decade as they are cheaper and less toxic than traditional phosphorescent transition metal complexes, lending to their application in biological fluorescence imaging and photodynamic therapy [1–6]. BODIPY (4,4-difluoro-4-bora-3a,4a-diaza-s-indacene) is an extremely versatile organic dye with strong visible-light absorption and high fluorescence quantum yields [7]. BODIPY's versatility arises from the broad tolerance of the corresponding aldehyde and pyrrole starting materials that can be used to install substituents on any of the 8 ring positions (Fig. 1) [7].

Additionally, the core is easily post-synthetically modified and allows the fine tuning of photophysical properties to tune the absorption maximum wavelength (λ_{max}) and modulate the emissive properties [8]. For these reasons, BODIPY derivatives have been employed as photosensitisers for the generation of singlet oxygen, which can be activated at lower energy wavelengths of light relative to transition-metal complexes [9–11].

Singlet oxygen ($^1O_2$) is the first electronic excited state of molecular oxygen, lying 94 kJ mol^{-1} above the triplet ground state ($^3\Sigma_g^-$). Despite the low energy gap, direct transition to the $^1\Delta_g$ state is forbidden by spin selection rules and requires triplet photosensitisation to occur. $^1O_2$ is a reactive oxygen species (ROS) and has unique reactivity for oxidation of organic compounds, such as [2 + 2] and [4 + 2] cycloadditions, Schenck-ene group transfer pericyclic reactions, and selective oxidation of

Electronic supplementary material The online version of this article (https://doi.org/10.1007/s41981-019-00067-4) contains supplementary material, which is available to authorized users.

✉ Filipe Vilela
F.Vilela@hw.ac.uk

[1] Institute of Chemical Sciences, School of Engineering and Physical Sciences, Heriot-Watt University, Edinburgh, Scotland EH14 4AS, UK

[2] Institute of Sensors, Signals and Systems, School of Engineering & Physical Sciences, Heriot-Watt University, Edinburgh EH14 4AS, UK

Published online: 13 February 2020

heteroatoms [12, 13]. The first report of photosensitised $^1O_2$ intentionally applied in organic synthesis was by Schenck and Ziegler in 1944, who used chlorophyll isolated from spinach leaves to photosensitise singlet oxygen for the synthesis of ascaridole, a natural product with application as a anthelmintic agent [14]. Since 1944, singlet oxygen has been frequently applied in the synthesis of natural products and pharmaceutically relevant agents [13]. Most notably it is used in the synthesis of artemisinin, an Nobel prize winning antimalarial drug produced on a tonnes-per-year scale [15, 16].

Despite the reduced toxicity of organic dyes, separation of the photosensitiser still remains an issue and often requires cumbersome purification procedures which add significant expense to industrial processes. A solution that overcomes these issues is the application of heterogeneous photosensitisers [17–19], which are insoluble and therefore can be easily separated from a reaction medium and recycled. However, heterogeneous photocatalysts are often less efficient due to mass transport limitations and poor penetration of light through the bulk of the material. Hence, development of heterogeneous photocatalysts has been identified as one of the main challenges within the field of photochemistry [20]. With this in mind, we have looked to develop an organic photosensitiser, covalently immobilised on a polymeric support, in order to attain a balance of advantageous properties from both homogeneous and heterogeneous photocatalysts.

Merrifield resins are typically random co-polymers of styrene and divinylbenzene (1–3%). The resins are co-polymerised with a functionalised monomer which provides a reactive site for chemical synthesis. The materials were developed by R. B. Merrifield for solid phase peptide synthesis, for which he was awarded the Nobel Prize in 1984 [21]. As these materials are lightly cross-linked, they swell by up to a factor of 6 in suitable organic solvents [22, 23], enhancing the interface between the material and reaction media. Additionally, the swelling significantly enhances the material transparency, allowing light to easily penetrate the entirety of the heterogeneous photosensitiser whilst retaining the ease of separation and recycling advantages. By using a solid support which is non-semiconducting, the photophysical properties of the catalyst are unaltered from the homogeneous analogue and the mechanism of photosensitisation can be directly compared.

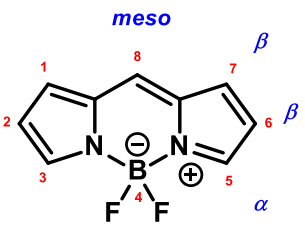

Fig. 1 Structure and IUPAC numbering/labelling convention of BODIPY cores

To overcome mass transport limitations and inefficient light penetration, we have turned to continuous flow chemistry for both material synthesis and photosensitisation reactions. Flow processes permit in-line spectroscopy such as UV-Vis, IR, mass spectrometry and NMR, which simplifies process optimisation and reaction monitoring with better reproducibility [24–28].

Immobilisation of porphyrin photosensitisers has been previously reported on Merrifield resins [29], polymer-supports [30, 31], and inorganic porous materials such as zeolites [32, 33], but have suffered from photobleaching and catalyst leaching due to instability of the catalyst or linker to photochemical conditions and have not taken advantage of continuous flow operation. Poliakoff and George *et al.* reported a variety of polymer-supported porphyrin photosensitisers for singlet oxygen oxidations in flow using super-critical CO_2 ($scCO_2$) as a reaction medium [34]. They found that covalently immobilised photosensitisers with amide linkages had the best long term stability and efficiency, but their materials did show steady decline in conversion over 6 h irradiation periods. Whilst $scCO_2$ is an attractive reaction medium for $^1O_2$ generation as it is miscible with oxygen, it requires high operating pressures and specialised equipment. Polymer-supported BODIPYs have also been previously reported, but typically on nanoscale materials for fluorescence imaging purposes and not photosensitisation [35, 36]. BODIPY has been applied for heterogeneous photosensitisation of singlet oxygen by incorporating the core as a repeat unit in conjugated porous polymer materials, as previously published by our group [10, 37].

Herein, we report a novel strategy for the post-synthetic modification of polymer substrates in continuous-flow using a mild oxidant, trichloroisocyanuric acid (TCCA), to generate ester-linked BODIPY photosensitisers. The polymer-supported ester-linked BODIPY was concurrently synthesised under batch conditions to compare the quality of materials produced. Both materials were fully characterised by solid state UV/Vis-, CP-MAS-^{13}C-NMR-, FTIR spectroscopies and elemental analysis. The homogeneous analogue of the polymer-supported BODIPY was synthesised as a reference to study the effect of the polymer-support and linker on the photophysical properties of the photosensitiser core. An unexpected side reaction, in which TCCA was able to chlorinate the BODIPY core, serendipitously yielded two new compounds which were isolated and found to be superior photosensitisers relative to the desired compound. The side reaction was entirely mitigated by performing post-synthetic modification in flow, as removal of impurities and reactants could be performed between steps in a 'one-pot' type synthesis. The homogeneous and polymer-supported BODIPYs were successfully applied as photosensitisers for the generation of singlet oxygen and subsequent conversion of α-terpinene to ascaridole. Photosensitisation in flow generally showed a significant rate enhancement over batch.

Heterogeneous photosensitisers were easily recycled and could be irradiated for a total of 96 h without significant loss of photosensitising ability. Flow rate and pressure optimisation was performed by employing an in-line benchtop NMR spectrometer. Additional material modification and flow conditions optimisation resulted in a 24-fold rate enhancement from the initial material and conditions.

Results and discussion

Materials and molecule synthesis

For this work we targeted 1,3,5,7-tetramethyl-8-*(p)*phenol substituted BODIPY (BDP-PhOH (**1**), Scheme 1) with the intention of utilising the phenolic hydroxyl group as the photocatalyst coupling site to generate an ester linkage between the polymer-support and BODIPY. The molecule was obtained by adapting a standard procedure previously used by our group, using 4-hydroxybenzaldehyde as a starting material (Scheme 1) [10]. Initially, a poor yield of 15% was obtained, so following an alternative literature report the synthesis was repeated and further modified to increase the solvent dilution by a factor of 6 which gave an increased yield of 34% [38], a more consistent yield expected for BODIPY synthesis. The authors did not discuss their higher dilution in the paper, but it seemed sensible due to the poorer solubility of 4-hydroxybenzaldehyde in dichloromethane relative to benzaldehyde, and to reduce the influence of impurities in this one-pot procedure.

As our Merrifield-resins were functionalised with formyl groups (PS-COH (**2**), Scheme 2) we looked to generate an acyl chloride intermediate (PS-COCl (**3**), Scheme 2), which would be activated towards nucleophilic attack of **1**, rather than oxidise to the carboxylic acid. The former approach avoids use of chromium-based reagents and maintains a metal-free strategy. De Luca *et. al.* reported trichloroisocyanuric acid (TCCA) as a mild oxidant and chlorinating agent for the in situ generation of benzoyl chloride for one-pot oxidation of aldehydes to esters [39]. This strategy was appealing as it avoided use of toxic alternative reagents, such as thionyl chloride, and maintained our metal-free synthesis objective with a cheap and mild oxidising agent. The polymer-supported ester-linked BODIPY (PS-Est-BDP, (**4**) Scheme 2) was synthesised following the procedure published by De Luca *et al.* [39], but adapted for continuous flow synthesis on a solid matrix (Scheme 2). **2** were purchased from Rapp Polymere GmbH, with 500–560 μm diameter and a 4-formylstyrene functional loading of 0.62 mmol/g. The dry resins were loaded into a transparent borosilicate glass column and fitted to a Vapourtec E-series flow chemical reactor. The resins were swollen and washed in dry, degassed dichloromethane for two hours by pumping the solvent through the fixed bed reactor before the solvent flask was replaced with reaction mixture. The outflow needle was placed in the same flask to continuously recycle the reaction media. The TCCA solution was replaced by a flask of fresh dichloromethane and used to flush residual TCCA trapped in the polymer matrix, before addition of the final solution containing **1**, triethylamine (NEt_3) and 4-dimethylaminopyridine (DMAP) to achieve the polystyrene-supported, ester-linked BODIPY material, **4**.

The material was purified by flushing the immobilised resins, **4**, with fresh solvents (dichloromethane/methanol/water/chloroform neat and mixtures) at elevated temperature and pressure (25–50 °C, 0–3 bar adjusted as necessary to prevent solvents boiling in the reactor) for 72 h. Purifying materials in flow has unique benefits as; *(i)* mass transport limitations also apply to the removal of impurities from the polymer matrix, *(ii)* back-pressure can be applied to heat solvents beyond their boiling points and facilitate the diffusion of solvent into the material, *(iii)* mixed solvent systems can be used for purification and *(iv)* no change in set-up is required between synthesis and purification. All these points are not achievable in a conventional Soxhlet extraction and therefore materials can be purified significantly faster. The purified material was an appealing deep-red colour and fluoresced bright green under long-wave UV irradiation. Swelling tests were performed and found to be consistent with the starting material, indicating that no unexpected cross-linking nor damage to the resins had occurred from the synthesis. When swollen in solvent, the resins became significantly lighter in colour and more transparent. The intensity of fluorescence was also greatly enhanced due to better light penetration through the expanded polymer matrix and potentially a reduction in non-radiative decay through energy transfer mechanisms, such as Förster resonance energy transfer (FRET), as the supported dye molecules become more spatially separated.

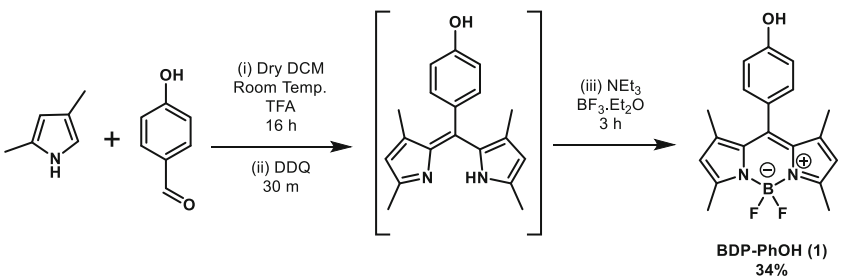

Scheme 1 Synthesis of BDP-PhOH (**1**)

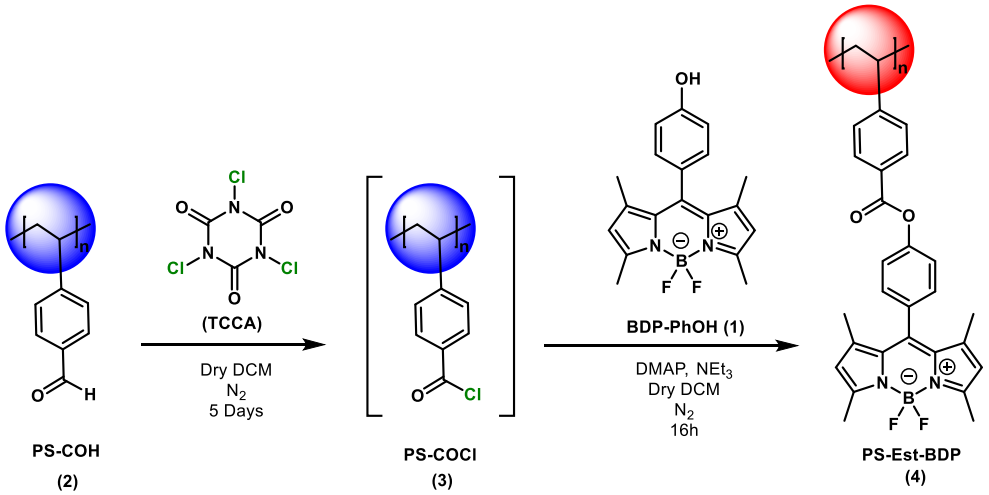

Scheme 2 Synthesis of polymer-supported, ester-linked BDP (**4**) from formyl polystyrene resins (**2**) via a TCCA generated benzoyl chloride resin intermediate (**3**)

Material **4** was concurrently produced using an identical procedure but under batch conditions for comparison. A round bottom flask and an overhead stirrer was used in place of the flow machine. The overhead stirrer was necessary to prevent the polymer resins from being damaged from attrition or mechanical grinding by a magnetic stirrer bar. The set up was significantly more cumbersome and a side-by-side comparison is displayed in the ESI (Figure S5). It was also noticed that despite using the overhead stirrer, the resins were partially damaged during the synthesis, as a fluorescent powder was observed in the filtration. The batch produced material, **5**, was purified by conventional Soxhlet extraction for 3 days with the same solvents to mimic the purification process of the flow machine. Functional loading of the polymer resins was quantified according to literature procedures [34, 40], by the percentage of nitrogen in CHN elemental analysis and UV-Vis spectroscopic analysis of the filtrate to quantify unreacted **1**. **4** were found to have a loading efficiency of 53% (0.33 mmol/g), significantly higher than **5** produced in batch with only 28% (0.17 mmol/g), demonstrating the greater efficiency of post-synthetic modification in flow through enhanced mass transport. A side-by-side comparison of the material's visual appearance under ambient and UV light is displayed below (Fig. 2). **5** had a similar green fluorescence but was also noticeably lighter in colour than the flow material, likely due to the lower coupling efficiency of the photosensitiser.

We attempted to synthesise the molecular analogue of the aryl-ester-linked BDP (Ph-Est-BDP (**6**), Scheme 3) following an identical procedure to that used to synthesise **4**, by exchanging the polystyrene resins for benzaldehyde as a molecular equivalent. Surprisingly, the reaction yielded none of the expected product, but rather the mono- and di-chlorinated derivatives, PS-Est-BDP-Cl (**7**) and PS-Est-BDP-Cl_2 (**8**). Collectively the isolated products accounted for 68% yield (50% **7**, 18% **8**). ^{1}H-NMR spectroscopic analysis of the impure fractions did show the presence of the desired **6**, but it was contaminated with **7** and proved extremely difficult to separate.

Clearly the 1.6 equivalent excess of TCCA in the reaction mixture was able to chlorinate a significant proportion of the ester product, even within the short reaction time of two hours. Electrophilic substitution of the 2- and 6- positions of BDP cores is a known reaction commonly performed with N-halogenated succinimides, but to the best of our knowledge this is the first example of TCCA chlorination of BDP [8, 10]. Despite not isolating the desired product, the protocol has provided a strategy for rapidly generating a library of photosensitisers from a single starting material, and pleasingly both chlorinated products are new compounds. To obtain the desired molecule **6**, the procedure was adapted, and benzoyl chloride was used directly to prevent chlorination (Scheme 4). **1**, DMAP and NEt_3 were dissolved in dry, degassed dichloromethane and benzoyl chloride was slowly added at 0 °C. After work-up, the product **6** was collected by recrystallisation from MeOH as a bright orange solid with 92% yield.

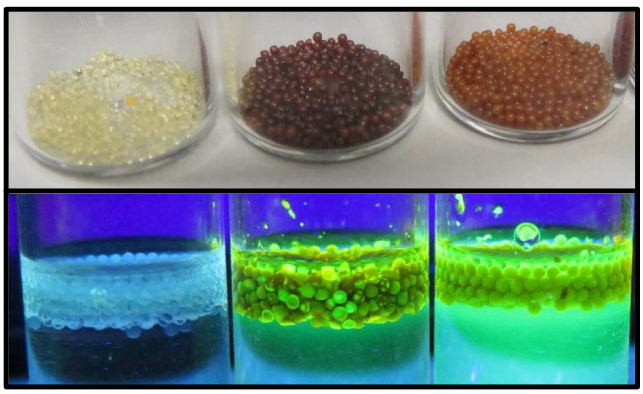

Fig. 2 Side-by-side comparison of PS-COH starting material (**2**), PS-Est-BDP produced in flow (**4**) and batch (**5**) from left to right, under ambient room lighting (top) and long wave UV irradiation (bottom)

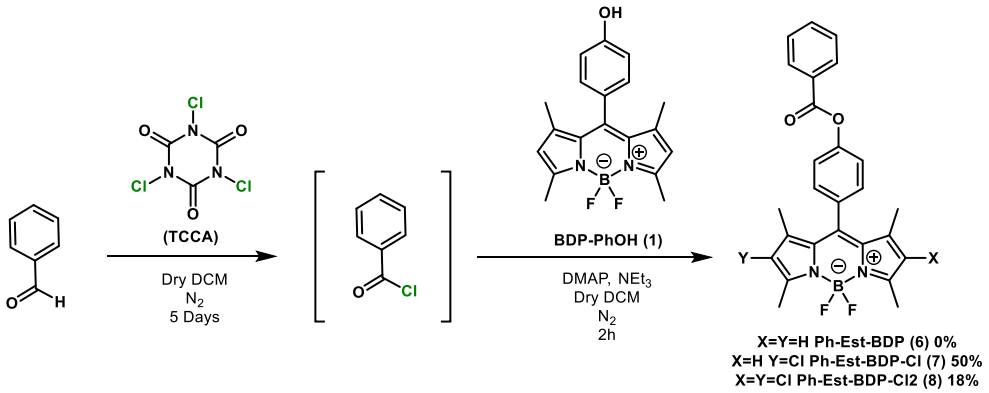

Scheme 3 Attempted synthesis of aryl ester BODIPY small molecule photosensitiser (**6**), yielding chlorinated products (**7**) and (**8**)

Single crystals were obtained for **7** and **8** by slow evaporation from acetone and analysed by x-ray diffraction to confirm their structures (Fig. 3). Crystal structure data is reported in the ESI (Section 6.8).

Spectroscopic characterisation

UV/Vis absorption and emission spectroscopies were employed to determine the optimal irradiation wavelengths for performing photosensitisation, as well as assessing the effect of the ester formation and chlorinations on the optoelectronic properties of the BDP core. **6** has been previously published with UV/Vis characterisation by Giordani *et. al.* and our results were found to be in good agreement [41]. Solutions of photosensitiser in acetonitrile solvent were produced and absorbance was measured across 800–350 nm wavelengths. The emission spectra and photoluminescence quantum yield were also measured in CH_3CN solvent using a spectrofluorometer (Edinburgh Instruments, FLS920) equipped with an integrating sphere. The absorption and emission spectra recorded are displayed below (Fig. 4) and relevant spectral data tabulated in Table 1. Individual spectra are displayed in the ESI (Figure S18-S26).

The absorption and emission λ_{max} value for **1** and **6** differs by only 1 nm which is within the error of measurements. This indicates that conversion of the hydroxyl to the phenyl ester has not significantly altered the optoelectronic properties of the BDP core. This suggests that conjugation does not extend from the BDP core through the *meso* substituted aromatic system, resulting in only subtle changes in the absorption and emission profile through inductive effects. This is also confirmed in the crystal structures as the phenyl ester is orthogonal to the BODIPY core due to the 1- and 7- methyl substituents sterically blocking the phenyl ring from a co-planar conformation in conjugation with the BDP core. In contrast, the 2- and 6-position chlorine substitutions produced a bathochromic shift of the absorption and emission profiles, indicating a reduction of the HOMO-LUMO energy gap. Monochloro substitution leads to a subtle shift in the λ_{max} of 11 nm and an appreciable reduction in the molar attenuation coefficient (ε). Dichloro substitution caused an additional 15 nm bathochromic shift of λ_{max}, 27 nm

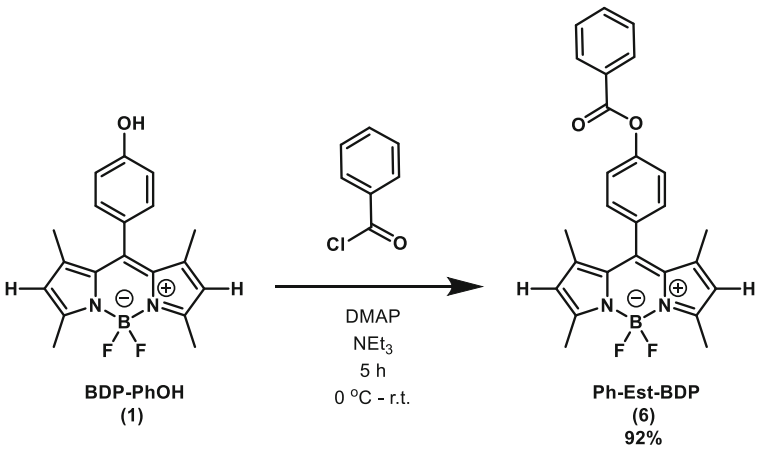

Scheme 4 Synthesis of Ph-Est-BDP (**6**)

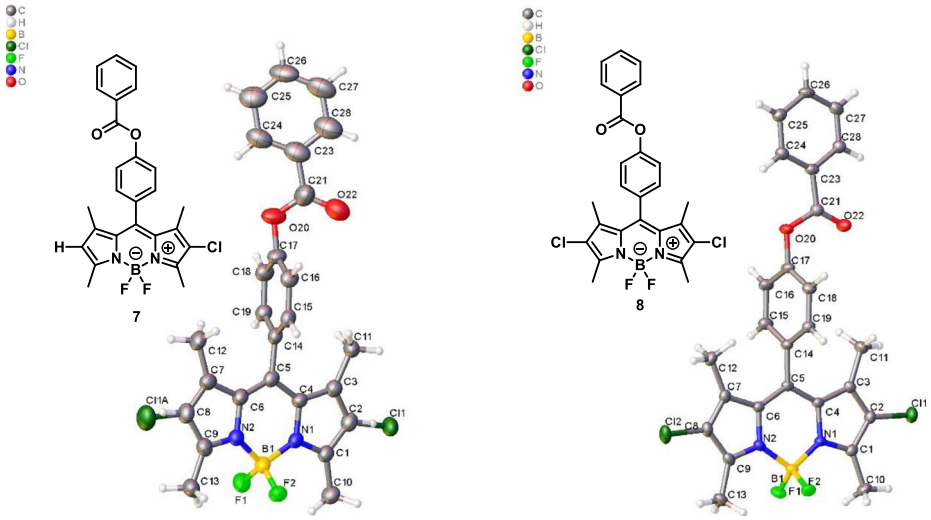

Fig. 3 Single crystal x-ray diffraction structure of **7** (left) and **8** (right) (CCDC deposit no. **7**: 1958564, **8**: 1958563). The **7** crystal has the chlorine atom disordered over the C2 and C8 sites in an 81:19 ratio

in total from the unchlorinated molecule and an even more significant reduction of ε. These results indicated that the polymer-supported BDP photocatalysts optoelectronic properties should not be significantly influenced by the polymer support, and the formation of a mixture of chlorinated BDP species on the polymer support could be identified by the solid-state UV/Vis absorption profile. All the homogeneous photosensitisers displayed emission spectra that were mirror images of their absorption spectra, with narrow Stokes shifts of ~20 nm.

To confirm the presence of the polymer-supported BDP, the materials were analysed by solid-state UV/Vis (SS-UV/Vis) spectroscopy (Fig. 5). A sample of resins **2**, **4** and **5** were ground to a powder using a mortar and pestle before recording SS-UV/Vis absorption spectra via an integration sphere. Pleasingly, the flow-produced resins displayed a sharp molecular-like absorption profile with λ_{max} at 505 nm, consistent with the λ_{max} of Ph-Est-BDP in toluene at 504 nm. The absorption profile displayed a smooth absorption edge

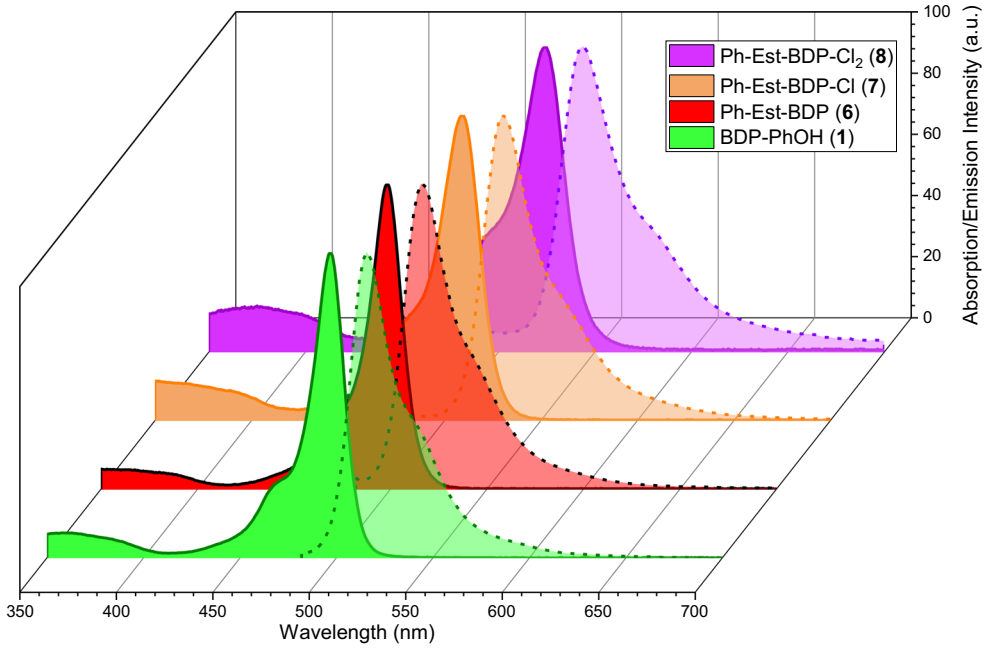

Fig. 4 Normalised UV/Vis absorption (solid line) and emission spectra (dashed line) between 350 and 700 nm of **1** (light purple), **6** (dark red), **7** (orange) and **8** (magenta), as measured in CH_3CN (1×10^{-5} M). Full spectra are displayed in the ESI (Section 6.3 and 6.4)

Table 1 Tabulated absorption and emission spectral data

[a]Photosensitiser	Absorption Maximum (λ_{max}) (nm)	Molar Attenuation Coefficient (ε) ($\times 10^3$ M^{-1} cm^{-1})	[c]0–0 Transition Energy ($E_{0,0}$) (nm, eV)	[d]Emission Maximum (λ_{max}) (nm)	Stokes Shift (nm)	Φ_F
BDP-PhOH (**1**)	497	127	505, 2.46	516	19	0.47
Ph-Est-BDP (**6**)	498	83.5	506, 2.45	516	20	0.55
Ph-Est-BDP-Cl (**7**)	509	66.1	519, 2.39	530	21	0.66
Ph-Est-BDP-Cl_2 (**8**)	524	38.9	533, 2.33	544	20	0.67

[a] In CH_3CN (1.0×10^{-5} M). [b] Measured as the intersect of the absorption and emission spectra, 1 eV = 1239.84 nm. [d] In CH_3CN (1.0×10^{-7} M)

which we suggest as evidence that a mixture of chlorinated products has not been produced. Conversely, the batch produced material **5** displayed a much less defined absorption profile with jagged features, lower relative absorption intensity and a bathochromically shifted absorption maximum, suggesting that chlorinated side products had formed. This demonstrates a unique advantage of post-synthetic modification on heterogeneous substrates in flow, as 'one-pot' type synthetic procedures can be performed with intermediate purification steps to remove impurities and starting materials that may lead to reaction inhibition and side-product formation.

The powdered samples were analysed further by FTIR spectroscopy to identify changes in the carbonyl stretch frequencies between the product and starting materials (Fig. 6). The formyl styrene aldehyde stretch was identified at 1699 cm^{-1} as a sharp peak with a small shoulder feature towards lower wavenumbers, and all other peaks were characteristic of polystyrene. In comparison, **4** and **5** showed a significant broadening of the carbonyl stretch frequency region, as well as a broadening of the signals where aromatic stretching frequencies and ester C-O-C vibrational modes are typically expected, concurrent with the successful formation of the ester linked BDP. The broad features of the carbonyl absorptions are likely due to multiple environments in the dry amorphous polymer modulating the stretch frequencies.

A sharp absorption peak at 1699 cm^{-1} emerging from the broadened carbonyl region was still present in materials **4** and **5**, potentially suggesting there are unreacted formyl styrene monomers still present in the polymer. Due to the amorphous nature of the polymer resins, it is expected that some functional groups will be trapped inside highly crosslinked regions of the polymer matrix and shielded from post-synthetic modification. Material characterisation by solid-state cross-polarisation magic angle spinning (SS-CP-MAS) ^{13}C-NMR spectroscopy was attempted but yielded no useful comparison for any of the samples because of the relative proportion of styrene and divinylbenzene to the BDP functionalised monomer, which equates to approximately 93% to 7% respectively. The spectra recorded are displayed in the ESI (Figure S14-S17).

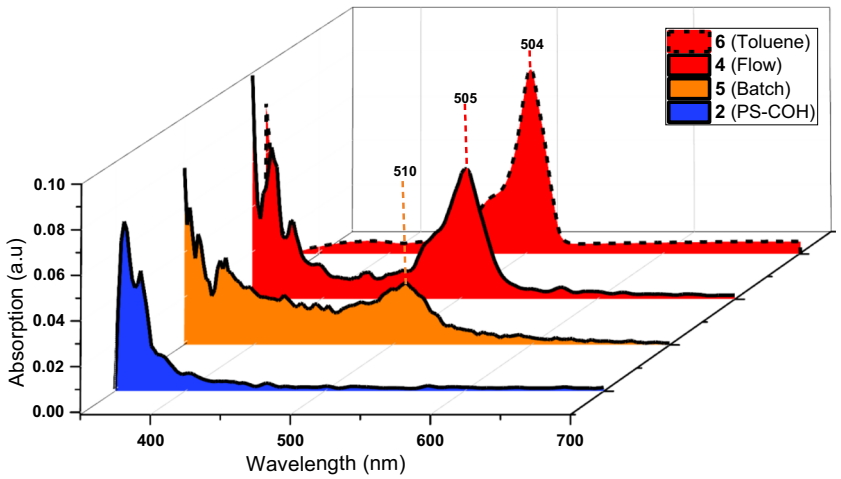

Fig. 5 Solid-state UV/Vis absorption spectrum of **2** (blue), **5** (orange) and **4** (red, straight line) measured using an integration sphere. The solution state absorption spectrum of **6** in toluene is shown for reference (red, dashed line)

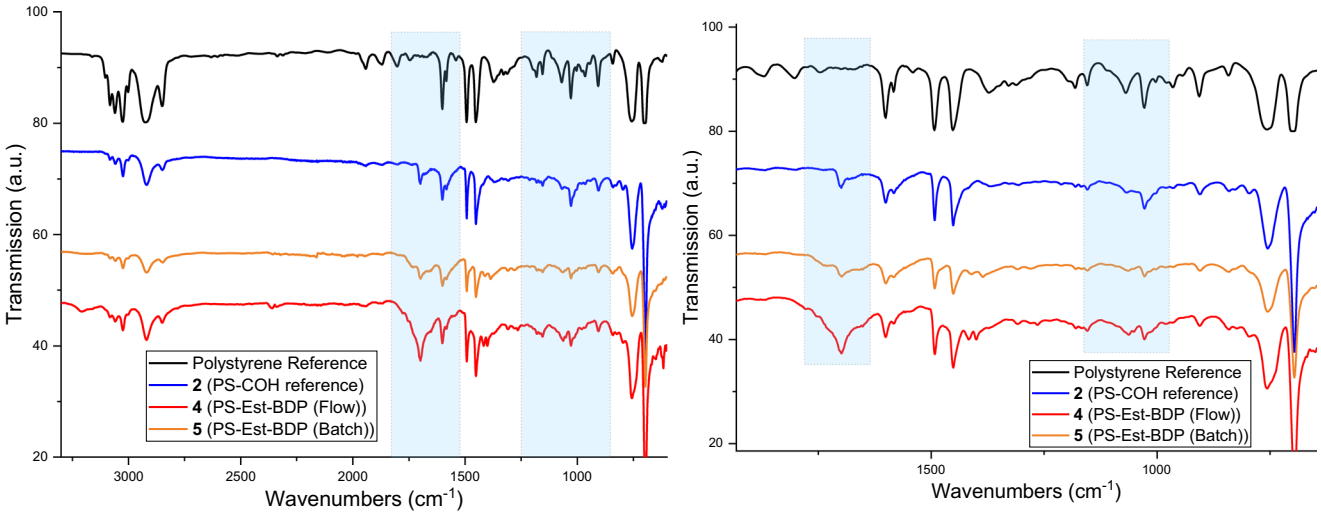

Fig. 6 FTIR spectra of materials **2**, **4** and **5** and a polystyrene reference (left). Regions between 1750 and 1550 cm^{-1} and 1150–925 cm^{-1} have been highlighted and magnified to emphasise changes in the carbonyl and aromatic transmission signals (right)

Singlet oxygen photosensitisation

We have chosen to use photosensitised $^1O_2$ oxidation of α-terpinene to ascaridole to develop and assess the photosensitising capabilities of our materials as the reaction has been well studied within our group and is easily assessed by ^{1}H-NMR spectroscopy, making it well suited to in-line NMR spectroscopic analysis [10, 42, 43]. The lifetime of singlet oxygen has a high dependency on solvent environment due to vibronic-energy coupling, ranging from 3.1 μs in H_2O to >309 ms in perfluorodecane [44]. We perform our reactions in $CHCl_3$ as it provides the longest singlet oxygen lifetime of common organic solvents (~229 μs).The reaction occurs by a concerted but asynchronous mechanism that is competitive with the Schenck-ene reaction – but for heterocyclic substrates the endoperoxide is formed exclusively [45]. The Schenck-ene hydroperoxide product of α-terpinene has not been observed, but *p*-cymene can form as a minor by-product via a type-I (radical based) photosensitised oxidation process (Scheme 5) [13, 44].

Batch reactions are performed in sample vials loaded with magnetic stirrer bars, placed on a magnetic stirrer plate and covered with a reflective enclosure to enhance

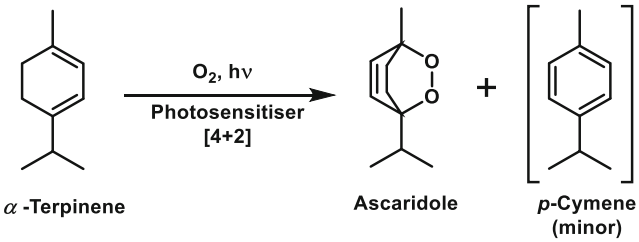

Scheme 5 Reaction of α-terpinene in the presence of singlet oxygen to form ascaridole, and minor product *p*-cymene

irradiation. The vials are placed at a fixed distance of 7 cm from a 500 nm LED array and irradiated for up to 24 h. Reactions in flow are performed with two almost identical set-ups for homogeneous and heterogeneous photosensitisers, differing only in the type of photochemical reactor used. A flow scheme for heterogeneous photosensitisation reactions is displayed below (Fig. 7) and the homogeneous equivalent is displayed in the ESI (Section 5.2). Homogeneous flow photosensitisation reactions are performed with a 10 mL coil of transparent PTFE tubing (1 mm ID). The reaction solution is placed in a covered round bottom flask sealed by a septum with an input and output needle connected to the Vapourtec flow machine. Solution is flown at 1 mL/min *via* peristaltic pumps to a T-junction, where it is mixed with a stream of air pumped at 1 mL/min by a second peristaltic pump. The air is saturated with $CHCl_3$ by employing a pre-bubbler to reduce evaporation of solvent. The T-junction generates a slug flow of reaction solution and air, which ensures the solution phase is saturated with oxygen and enhances mixing. For heterogeneous photosensitisation reactions, the same set-up is employed except the photosensitiser resins are immobilised in a fixed bed reactor in place of the coil, and a back pressure regulator is included to control pressure. In both flow systems, a Nanalysis 60e benchtop spectrometer (60 MHz) adapted for flow chemistry, could be incorporated to the system between the solvent pump (pump A) and the T-junction for in-line monitoring of reaction conversion.

Samples are extracted periodically and concentrated *in vacuo* to perform crude ^{1}H-NMR spectroscopy analysis. The alkene protons of ascaridole are shifted downfield from α-terpinene and can be integrated to assess conversion. Heterogeneous photosensitisation reactions were performed

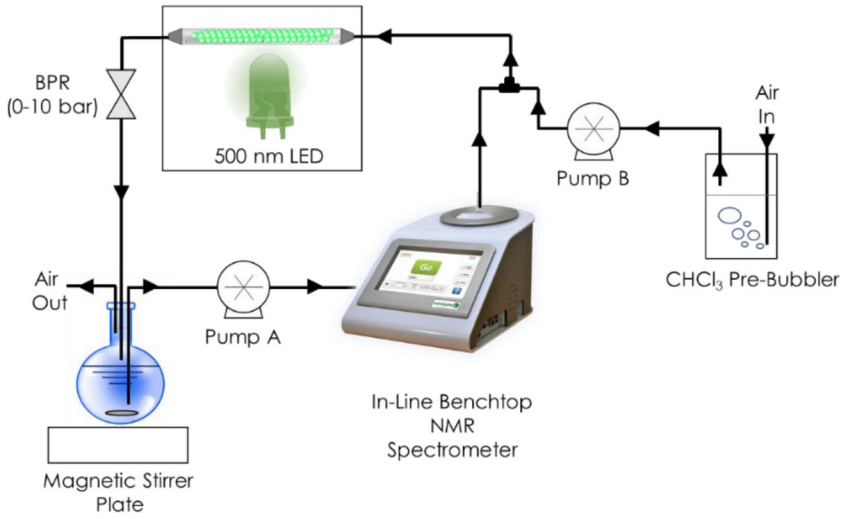

Fig. 7 Representative flow scheme for heterogeneous photosensitisation reaction with a fixed-bed column reactor with an in-line Nanalysis 60e benchtop spectrometer

with 200 mg of resins, equivalent to ~5 mol% of polymer-supported photosensitiser. The results are displayed in Table 2 and show a peak conversion of 58% in 24 h after 2 cycles. The first cycle of the catalyst provides lower conversion, but this could be due to the catalyst requiring time to prime in the reaction mixture which is negated in subsequent cycles. Similar results have been reported by Poliakoff *et. al.* with polymer-supported photosensitisers in super critical CO_2

Table 2 Heterogeneous photosensitisation of singlet oxygen results

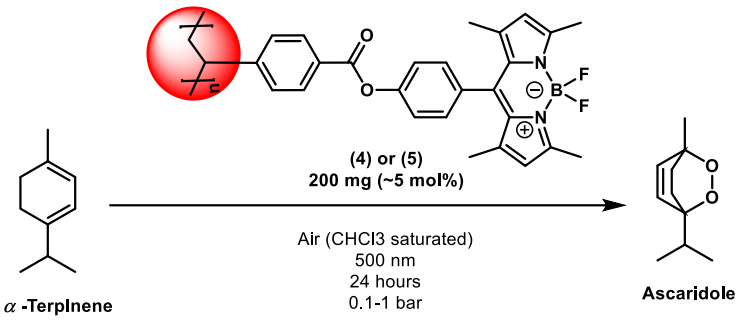

[a]Entry	Polymer-Supported Photosensitiser	Reaction Time	Batch/Flow Reaction	Conversion (%)	Cycle Number (Total Irradiation in hours)
1	**4**	24h	Flow	27	1 (24)
2	**4**	24h	Flow	39	2 (48)
3	**4**	24h	Flow	58	3 (72)
4	**4**	24h	Flow	38	4 (96)
5	**4**	24h	Batch	10	1 (24)
6	**4**	24h	Batch	22	2 (48)
7	**4**	24h	Batch	26	3 (72)
8	**4**	24h	Batch	25	4 (96)
9[b]	**5**	24h	Batch	25	1 (24)
10[b]	**5**	24h	Batch	21	2 (48)
11[b]	**5**	24h	Batch	13	3 (72)
12[b]	**5**	24h	Batch	8	4 (96)
13[c]	**4**	24h	Flow	29	1 (24)

[a] Reaction conditions: α-terpinene (1 mmol/15 mL $CHCl_3$), heterogeneous photosensitiser (~5 mol%), 500 nm LED irradiation, air. [b] PS-Est-BDP batch material, **5**, used under standard conditions for comparison with flow material.[c] Pure oxygen used in place of lab air

($scCO_2$) [34]. Heterogeneous photosensitisation in flow shows an almost 3-times greater conversion than the equivalent batch reaction before any optimisation of flow rate or pressure of the flow system. A series of control experiments were performed to confirm that the polystyrene support was not interfering with the singlet oxygen photosensitisation, displayed in Table 3.

We elected to use lab air for our reactions as an operationally simple and cheap source of molecular oxygen. Using pure oxygen is known to greatly enhance the rate of liquid phase oxidations as oxygen, which is poorly soluble in most organic solvents, is no longer in competition with other gases from the atmosphere for dissolution [46]. This is demonstrated in Table 2 (entry 13) and Table 4 (entry 11), where using pure oxygen led to a 5% and 25% rate enhancement respectively, over the same conditions with lab air. Additionally, pure oxygen removes variability associated with air caused by changes in weather or location. However, use of pure oxygen is not preferred for industrial settings due to the hazards associated with forming a potentially explosive mixture of volatile organics and O_2 in a reactor's headspace, and typically 'synthetic air' (<10% O_2 in N_2) is preferred [46].

The resins produced in flow, **4**, can be irradiated for up to 96 h without loss of photosensitising ability and relatively consistent conversions under batch and flow reaction conditions (Fig. 8). The batch resins, **5**, were only tested in batch photosensitisation reaction as we thought it was fair to assume that a flow reactor would not be available if the synthesis was restricted to batch. The **5** resins initially performed surprisingly well, comparable to the flow system in the first reaction cycle. However, unlike **4**, the conversion in subsequent cycles rapidly declined to less than 8% conversion in the final 24 h cycle. We propose this is due to a combination of *(i)* photosensitiser cleaving from the polymer-support over time, and *(ii)* inefficient purification of the batch material by Soxhlet extraction, leaving a significant amount of **1** trapped in the resins to leach into reactions, leading to an observed initial enhanced efficiency that rapidly decreases from repeated purification between reactions.

4 was re-analysed by CHN elemental analysis, SS-CP-MAS-^{13}C-NMR, SS-UV/Vis and FTIR spectroscopies after the 96 h of irradiation period to identify any changes to the material. The material had become noticeably lighter in colour, and a clear decrease in SS-UV/Vis absorption intensity relative to the baseline suggested that supported BDP was becoming deactivated or cleaved over time under the reaction conditions (Fig. 9). Additionally, the FTIR spectra showed a similar decrease in absorption intensity of aromatic and carbonyl regions. CHN analysis revealed that only 10% of the initial nitrogen content was still present in the beads, confirming that the BDP was being cleaved from the polymer-support over time. Reaction solutions were analysed by UV-Vis spectroscopy to quantify the amount of BODIPY being cleaved from the resins in each cycle. It was found that approximately 9–41 ($\times 10^{-5}$) mmol was present in the reaction mixtures. The amount of BODIPY cleaved in each cycle was not consistent but the general trend showed a decline in each subsequent cycle, and that reactions that were terminated by a timer in the middle of the night and left in the dark until being worked up the next day also typically had higher concentrations of cleaved BDP, potentially implicating the acidic chloroform solvent as an additional source of linker cleavage.

After the initial testing of the polymer-supported photosensitisers, the homogeneous photosensitisers were tested to compare efficiency. As the homogeneous systems have a much greater exposure to oxygen and light, reactions were performed with 1 mol% of photosensitiser. Results are displayed below in Table 4, along with conversion versus time traces (Fig. 10).

To identify potential decomposition or cleavage of the catalyst and aryl ester linkage by light and singlet oxygen, samples **6** were irradiated under aerobic and nitrogen atmospheres

Table 3 Singlet oxygen control experiments

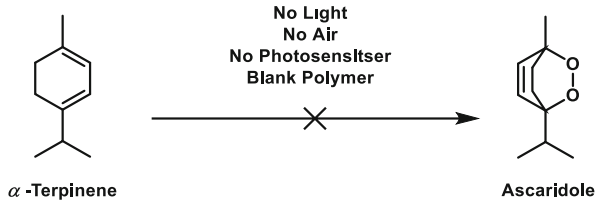

[a]Entry	Deviation from standard conditions	Irradiation λ (nm)	Time (hours)	Batch/Flow	Conversion (%)
1	No light	-	5	Flow	0
2	**2** used as photosensitiser	500	5	Batch	0
3	No air (nitrogen atmosphere)	500	5	Flow	0
4	No photosensitiser	500	5	Flow	0

[a] Reaction conditions: α-terpinene (1 mmol/15 mL $CHCl_3$), Photosensitiser (5 mol%), LED irradiation, air

Table 4 Homogeneous photosensitisation of singlet oxygen results

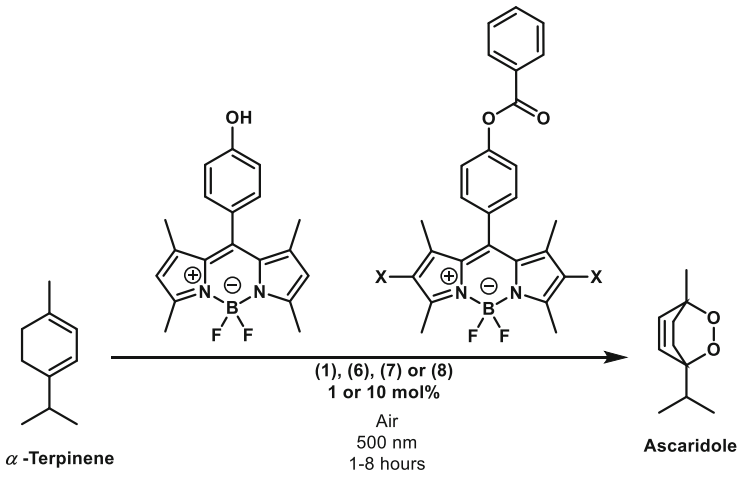

[a]Entry	Photosensitiser (mol%)	Irradiation λ (nm)	Time (hours)	Batch/Flow	[b]Conversion (%)	Zero-Order Rate Constant (k, M h^{-1})
1	**1** (1)	500	8	Batch	27	0.002
2	**6** (1)	500	8	Batch	35	0.003
3	**7** (1)	500	3	Batch	>99	0.025
4	**8** (1)	500	3	Batch	>99	0.023
5	**1** (1)	500	3	Flow	40	0.009
6	**1** (10)	500	3	Flow	66	0.014
7	**6**(1)	500	3	Flow	69	0.016
8	**6**(10)	500	3	Flow	>99	0.021
9	**7** (1)	500	1.16	Flow	>99	0.056
10	**8** (1)	500	1	Flow	>99	0.076
11[c]	**8** (1)	500	0.7	Flow	>99	0.095

[a] Reaction conditions: α-terpinene (1 mmol/15 mL $CHCl_3$), Photosensitiser (1/10 mol%), 500 nm LED irradiation, air. [b] Analysed by crude ^{1}H-NMR spectroscopy with a 300 MHz instrument. [c] Pure O_2 used in place of air

and monitored by ^{1}H-NMR and UV/Vis spectroscopic analysis. The ^{1}H-NMR spectrum of both samples remained relatively consistent in terms of signals and relative integrals over 24 h of irradiation. However, the sample irradiated under aerobic conditions displayed a gradual colour change from bright yellow to a darker yellow/brown. The sample under nitrogen remained unchanged in appearance. Irradiation was continued for a further 24 h, at which point the ^{1}H-NMR integrals of the aromatic region began to deteriorate, but no new signals were observed. The absorption maximum of the irradiated **6** had decreased from 84 to 66 ($\times 10^3$ M^{-1} cm^{-1}) (Fig. 11). The mechanism could not be identified, but in combination with the recycling experiments of **4,** we suggest that the ester linkage is not stable to either $^1O_2$ or potentially superoxide radicals that are sometimes produced by type-I photosensitisation processes [13, 44].

Mechanistic and photophysical rationalisation of photosensitisation efficiency

All of the homogeneous reactions followed a zero-order kinetic profile, which has been previously observed for singlet oxygen oxidations by Poliakoff *et. al* [47]. The mechanism of singlet oxygen photosensitisation is well known and represented in Scheme 6. The key steps are the formation of a triplet electronic excited state (T_1) of the photosensitiser by intersystem crossing (ISC) from the singlet excited state (S_1) following absorption of a photon. The triplet state then undergoes a triplet-triplet annihilation (TTA) energy transfer process to result in the formation of ground state photosensitiser and singlet oxygen, which readily occurs as the process conserves electronic angular momentum. TTA is in competition with phosphorescent radiant decay ($h\nu_p$) to the ground state but

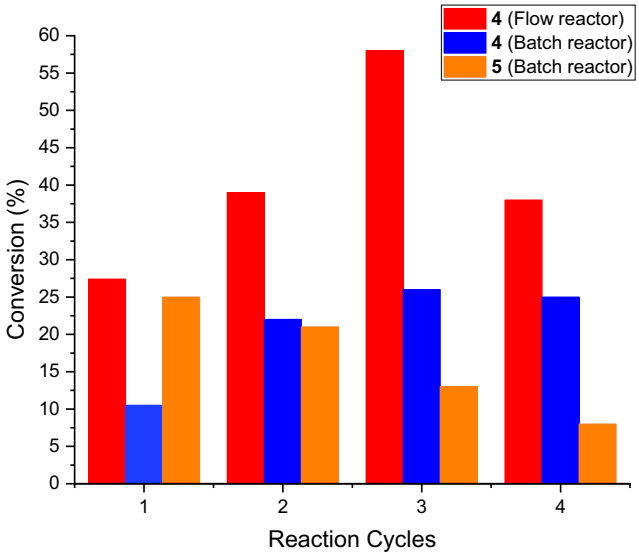

Fig. 8 Conversion of α-terpinene to ascaridole over time with **4** and **5** heterogeneous photosensitisers in the flow reactor (red) and in batch (blue/orange). Conversion monitored by ^{1}H-NMR spectroscopy

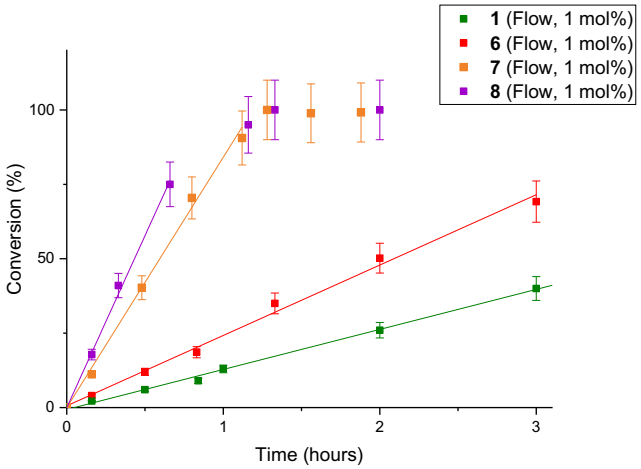

Fig. 10 Conversion of α-terpinene to ascaridole over time for homogeneous photosensitisers in flow (1 mol%). Straight lines represent linear regression fits to zero-order kinetics model. Error bars indicate potential error associated with ^{1}H-NMR integration values

typically occurs on a shorter time scale. The zero-order kinetic profiles indicate that ISC is the rate-determining step, which is confirmed by the change in rate when the molar% of photosensitiser is varied without changing the amount of oxygen present in the system.

As expected, the homogeneous systems were significantly more efficient than the heterogeneous photosensitisers. Despite the absorption properties of **1** and **6** being very similar, the formation of the aryl ester linkage led to an increase in photosensitisation efficiency. The *meso*-substituent of BODIPY dyes is known to influence photophysical properties of the core through photoinduced electron transfer (PET) processes [7, 38]. If either of the *meso*-substituents frontier molecular orbitals are within the BODIPY core HOMO-LUMO energy gap, an intramolecular electron donor-acceptor regime is formed, providing a non-radiative decay pathway and diminished fluorescence (Fig. 12).

1 has previously been shown to undergo PET processes, as fluorescence is significantly quenched when the phenol hydroxyl group is deprotonated [38, 48]. Due to the higher fluorescence quantum yields and photosensitisation efficiency of **6**, we propose the aryl ester linkage has separated the *meso*-substituents frontier molecular orbital (FMO) energies from the BODIPY core, reducing non-radiative decay which in turn extends the excited state lifetime and presents more opportunity for ISC events. Addition of chlorine atoms to the BDP core greatly increased the photosensitisation efficiency, with **8** achieving full conversion in flow within one hour. This can also be rationalised by a reduction in PET effects, as the Cl atoms reduce the HOMO-LUMO energy gap of the BDP core

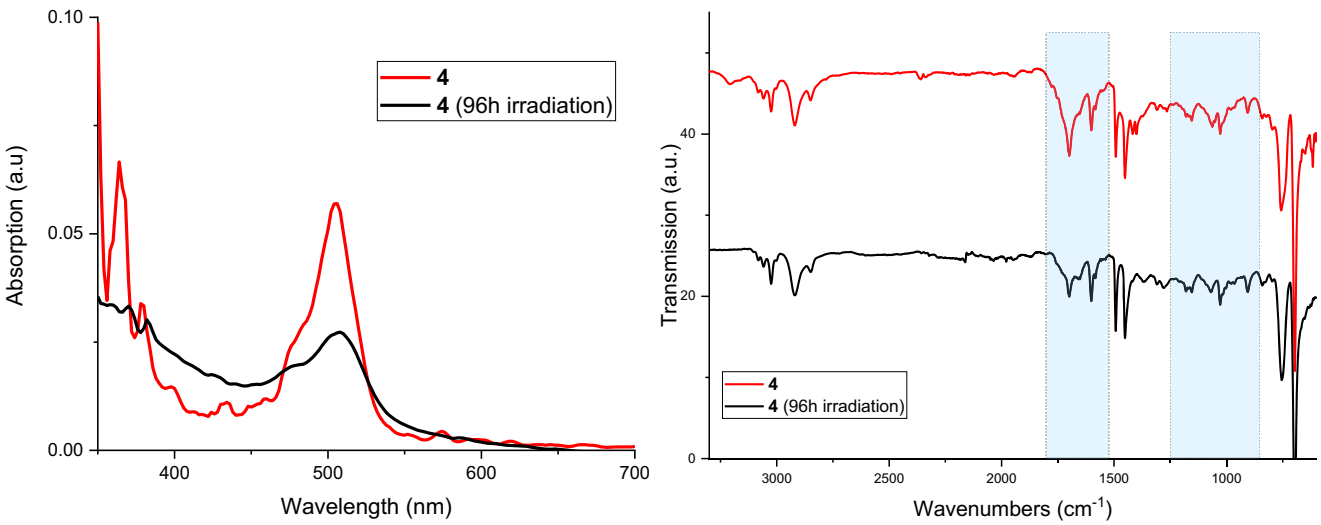

Fig. 9 Comparison SS-UV/Vis (left) and FTIR (right) spectra of **4** material before and after 96 h of irradiation under singlet oxygen conditions

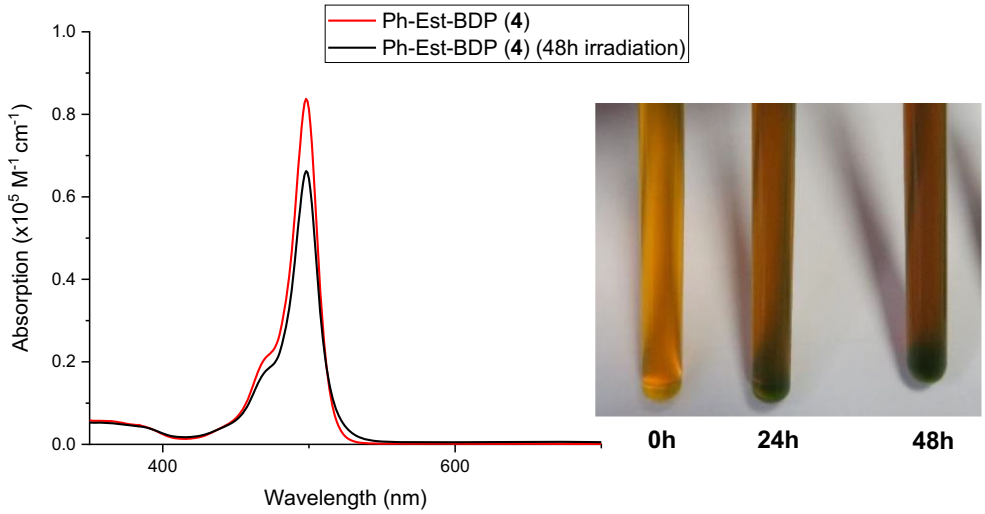

Fig. 11 Change in absorption intensity (left) and visual appearance (right) of **6**, irradiated for 48 h under aerobic conditions in flow

which is confirmed by the bathochromic shift in absorption maximum of the chlorinated compounds. Additionally, the higher order orbital angular momentum of period three elements can provide a subtle heavy atom effect through spin-orbit coupling of electrons which facilitates ISC, as shown by Jacquemin *et al.* with thiophene fused BODIPYs [49].

In-line ^{1}H-NMR spectrometer reaction monitoring and process optimisation

To show the dependency of light in the homogeneous reactions, a control experiment was performed in which the LED was cycled on and off every 20 min during a reaction under

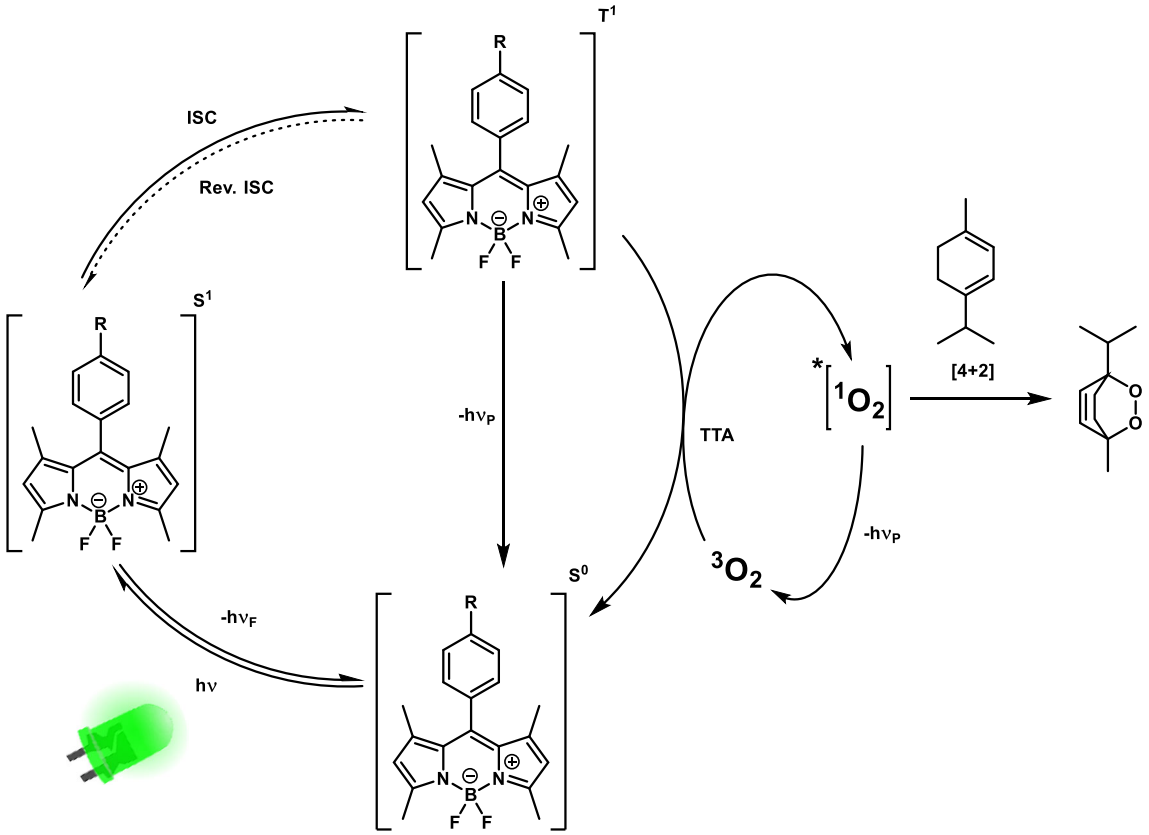

Scheme 6 Mechanism for the photosensitisation of singlet oxygen with homogeneous and polymer-supported BODIPY derivatives and subsequent [4 + 2] Alder-ene cycloaddition of singlet oxygen and α-terpinene to yield ascaridole

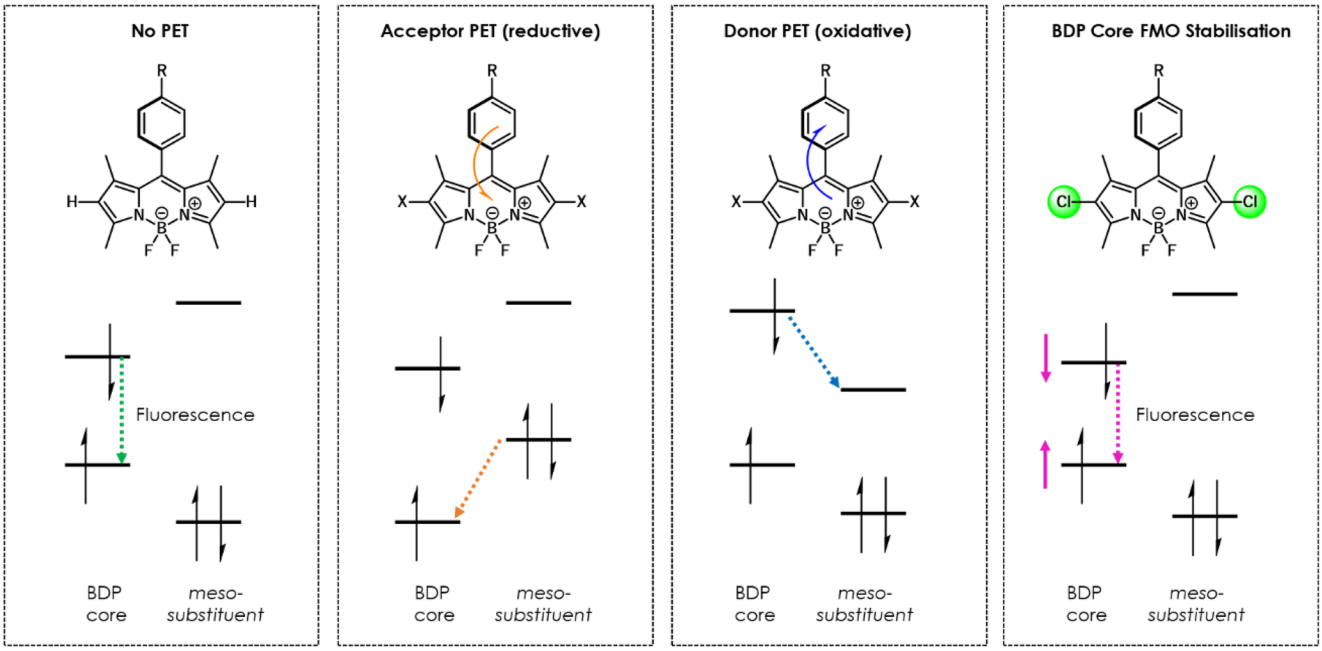

Fig. 12 Potential non-radiative decay pathways via PET with the *meso*-substituent of the BODIPY core. Figure adapted from Burgess *et. al.* [7]

standard conditions in flow with 1 mol% of **6** and deuterated chloroform solvent. The reaction conversion was monitored by in-line NMR spectroscopy and the reaction conversion trace is displayed below (Fig. 13). The periods of no irradiation, represented by grey columns, show a consistent plateau in the reaction conversion until 350 min where the reaction has reached completion. The rate of conversion in light periods is very consistent, showing that the reaction is still following zero-order kinetics in deuterated chloroform.

In order to optimise the conditions of the heterogeneous flow photosensitisation process, an in-line Nanalysis-60e benchtop NMR (60 MHz) spectrometer was employed to monitor reaction conversion with heterogeneous photosensitisers at varied flow rate and pressure (Fig. 14).

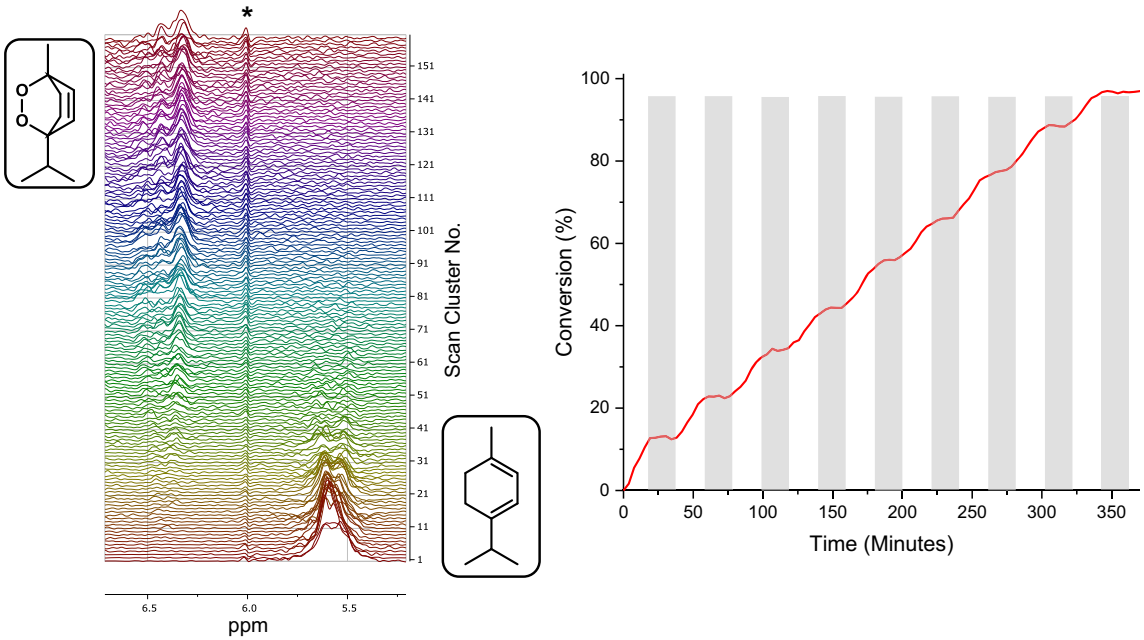

Fig. 13 Conversion of α-terpinene to ascaridole under standard flow conditions with **6** (1 mol%), monitored by in-line ^{1}H-NMR spectroscopy. The LED light source was cycled on and off every 20 min during the reaction, grey boxes represent periods of no irradiation. A smoothing function was applied in the data processing to show the data trend more clearly. * indicates a ^{1}H-NMR signal from the photosensitiser

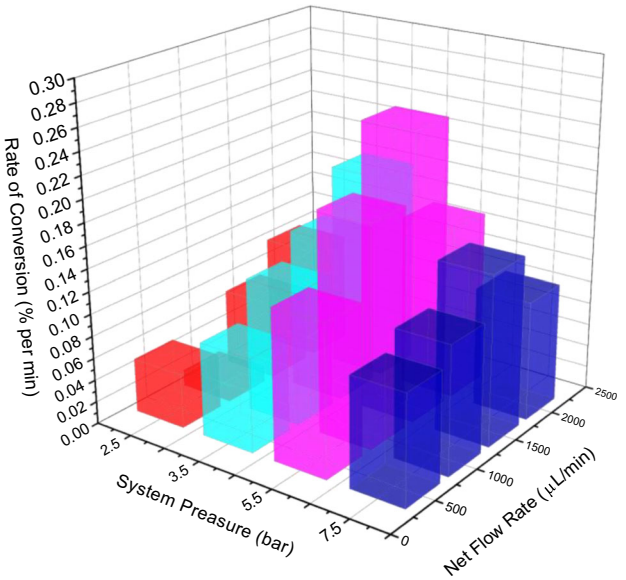

Fig. 14 Flow rate and pressure optimisation for conversion of α-terpinene to ascaridole, obtained using an in-line benchtop NMR spectrometer

The column reactor was packed with 500 mg of **4** and standard reaction conditions were applied, except for using deuterated chloroform as the solvent to be compatible with the in-line benchtop NMR spectrometer. The flow rate of reaction media and air was maintained at a 1:1 ratio for consistency. Flow rate was kept consistent while pressure was varied using a back-pressure regulator component of the Vapourtec flow machine. The material was irradiated at each condition for 50–100 min until a steady state of conversion had been achieved. The resins were washed between each flow rate series and replaced with fresh reaction media. Samples were periodically taken and referenced against a 300 MHz NMR spectrometer, and it was generally found that the benchtop NMR integral values were within 5–10%. After monitoring a series of conditions, the system was returned to the initial starting conditions to ensure the same rate was obtained, and hence the photosensitiser material had not deteriorated over the course of the experiment.

Flow rate was found to have a subtle effect on the rate of conversion, with 1500–2000 μL/min net flow rate generally being optimal across all pressures. Pressure had a more substantial effect on conversion rate, increasing the conversion per minute by a factor of 5 between 2.5 and 5.5 bar at 1500 μL/min. It was observed that at 5.5 bar, the slug flow of air and solvent became completely miscible, leading to a single phase of oxygen enriched $CDCl_3$. The formation of a single phase overcomes mass transport of oxygen in the system and significantly enhances the rate of reaction. Increasing the pressure further to 7.5 bar had an inhibitory effect on the conversion rate, which we propose is caused by compression of the polymer resin materials reducing accessibility to the photosensitiser. It should be noted that the rate values measured are not absolute due line broadening making accurate integration of this system difficult, however the data obtained showed very clear trends across all experiments that permitted the optimal conditions to be interpreted. The same optimisation experiment was performed for oxygen flow rate by applying the by applying the optimised pressure of 5.5 bar and liquid flow rate (750 micro liters/min) while varying the flow rate of air independently (Fig. 15).

Increasing the flow of air from 1 to 3 mL/min had a significant enhancement on the conversion rate, indicating that the solubility of oxygen under the standard conditions was a significant limiting factor in the reaction. At 4 mL/min, the increased volume of air became immiscible with the chloroform, forming a biphasic flow. This led to the formation of air pockets in the column reactor which forced solution through the catalyst bed non-uniformly and prevented efficient contact of the solution with the supported photosensitiser.

Post-synthetic material modification and optimisation

Considering the results obtained for the homogeneous photosensitisers, it was decided to modify the **4** resins further to form the polymer-supported, ester-linked, dichlorinated BDP species (**9**, Scheme 7), to enhance the materials photosensitising efficiency. TCCA was trialled as a chlorinating agent, using **6** as a model compound in dry dichloromethane. Chlorination products were observed by TLC, but amongst a complex mixture of other species. Isolation via column chromatography was attempted but no product or starting material was recovered. It is assumed the oxidising potential of the reagent was resulting in decomposition of the BDP core as none of the fractions collected were fluorescent. Further studies are required to identify the mechanism of decomposition, but this further reinforces the benefits of post-

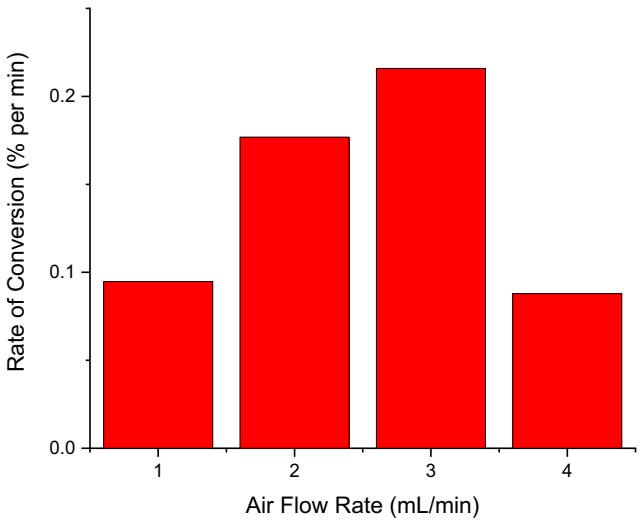

Fig. 15 Air flow rate optimisation of α-terpinene to ascaridole conversion with **4** (500 mg), obtained using an in-line benchtop NMR spectrometer

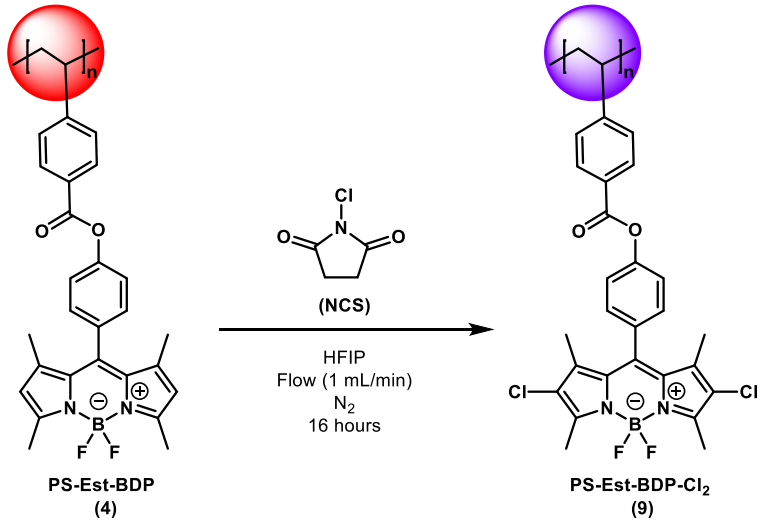

Scheme 7 Post-synthetic modification of **4** with NCS in flow to yield **9**

modifying materials in flow versus batch and provides additional rationale for the poorer loading and efficiency of the material produced in batch, **5**. To overcome this issue, we turned to an alternative and well-established method of halogenating BODIPYs with N-halogen succinimide in 1,1,1,3,3,3-hexafluoroisopropanol (HFIP) solvent, as reported by Wei *et al.* (Scheme 7) [50]. A 4-equivalent excess of N-chlorosuccinimide dissolved in HFIP was flown through a column packed with **4** for 16 h, washed and analysed by SS-UV/Vis and FTIR spectroscopy (Fig. 16).

The new chlorinated material, **9**, showed a broader absorption with a λ_{max} shifted to 523 nm, similar to the molecular analogue **8** (c.f. λ_{max} - 524 nm CH_3CN, 531 nm toluene). The broad absorption profile indicates that a mixture of BDP-H_2, -Cl and -Cl_2 photosensitisers are likely present on the material, despite the large excess of NCS used. The FTIR spectrum showed no significant changes from the parent material, showing the NCS and HFIP solvent had not affected the polystyrene support. The material was tested for singlet oxygen production under the initial standard conditions for direct comparison with the parent resin **4,** and then under the optimised conditions established with the in-line NMR spectrometer (Fig. 17).

The chlorinated material **9** showed a remarkable 8.5 times rate enhancement over its parent material under the initial standard reaction conditions, achieving >90% conversion in less than 6 h. Under the optimised conditions established with the

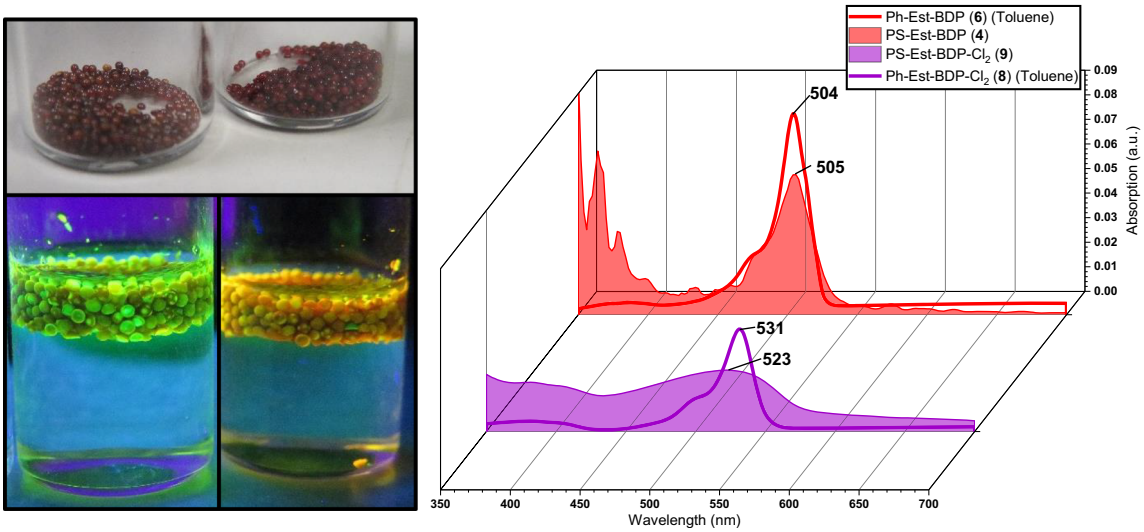

Fig. 16 Photographs of **4** (left) and **9** (right), dry under ambient visible-light (top) and swollen in DCM under UV irradiation (bottom). Right shows change in solid-state UV/Vis absorption from **4** to **9**. The Solution state spectra of **6** and **8** in toluene are superimposed on the material spectra as solid lines for reference

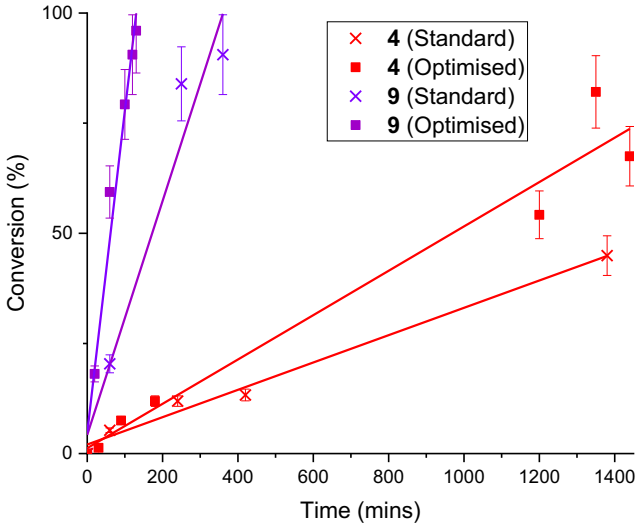

Fig. 17 Conversion traces of α-terpinene to ascaridole with **4** and **9** heterogeneous photosensitiser materials in flow under standard (cross markings, 0 bar, 1 mL/min air + solution) and optimised (square markings, 5.5 bar, 750 μL/min solution +3 mL/min air) conditions in $CHCl_3$

benchtop NMR, the rate of conversion was further increased by a factor of 3, and a total factor of 24 from the rate of the initial material under standard conditions. The overall space-time yield (STY) for the optimised system was calculated as 5 mmol L^{-1} min^{-1}. Material **9** was recycled five times under the optimised flow conditions for a total of 12.5 h irradiation and displayed a rapid decline in photosensitisation efficiency, although still significantly more efficient than material **4** and comparable to the initial performance before conditions optimisation (Fig. 18). It's likely that the greater efficiency of singlet oxygen photosensitisation has resulted in accelerated cleavage of the BODIPY photosensitiser from the support material. To assess this, we analysed the reaction mixtures by UV/Vis

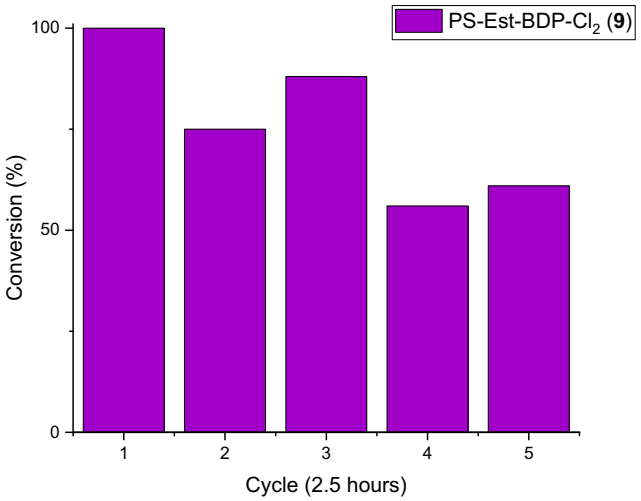

Fig. 18 Conversion of α-terpinene to ascaridole by recycling **9** heterogeneous photosensitiser material in flow under optimised conditions (5.5 bar, 750 μL/min solution +3 mL/min air) in $CHCl_3$

spectroscopy as previously performed with material **4** and found 1.8–8.1 × 10^{-5} mmol present in the solutions, corresponding to between 0.006–0.025% of the supported photosensitiser. The used material **9** was analysed by solid-state UV/Vis and no changes to the materials absorption spectrum were identified, suggesting that it is not the photolysis of the chlorine atoms that is leading to a reduction in efficiency.

In summary, we have established a mild protocol for the formation of aryl ester immobilised photosensitisers on Merrifield resins in continuous-flow and demonstrated the superior quality of materials produced in flow over conventional batch synthesis. Utilising a linker strategy through a position of the molecule that was not in conjugation with the photosensitiser core avoided altering the molecular optoelectronic properties, allowing the polymer-supported BDP to be identified easily by UV/Vis spectroscopy. Despite being non-conjugated, the support and linker was found to significantly enhance photosensitisation efficiency through reducing PET effects identified in the molecular analogues. An unexpected side-reaction led to the isolation of two novel compounds and demonstrated the ability to easily fine tune the optoelectronic properties of BODIPY cores to enhance photosensitisation efficiency. The polymer-supported photosensitiser was post-synthetically functionalised a second time to obtain the immobilised optimal photosensitiser, which displayed a remarkable 8.5-times enhancement in photosensitisation efficiency of the material. In-line ^{1}H-NMR spectroscopy was used to optimise the flow rate and pressure of the system, resulting in an overall 24-fold enhancement of singlet oxygen photosensitisation from the initial material and conditions, by enhancing the solubility of oxygen in chloroform at higher pressures. The heterogeneous photosensitisers sustained photosensitising ability after 96 h of irradiation, however leaching of the polymer-supported BDP was evident from photostability studies. The findings of this work have presented polymer-supported photocatalyst design principles such that our group is now considering the development of new Merrifield resin supported photocatalysts and immobilisation strategies for enhanced photocatalysis efficiency and photostability.

Experimental

Detailed experimental information of material synthesis, molecular synthesis and photosensitisation reaction set-ups and procedures can be found the ESI, section 1–4.

Acknowledgements We acknowledge Vapourtec Ltd. and Nanalysis Corp. for their valuable technical support. We would like to thank the Engineering and Physical Sciences Research Council, Heriot-Watt University and CRITICAT Centre for Doctoral Training for financial support [Ph.D. studentship to C.G.T; Grant code: EP/L014419/1].

C.G.T would like to thank Eve M. MacDonald, Keith M. Scott and the G. Barker Group (Heriot-Watt University) for helpful discussions.

Compliance with ethical standards

Conflict of interests On behalf of all authors, the corresponding author states that there is no conflict of interest.

References

1. Romero NA, Nicewicz DA (2016) Organic photoredox catalysis. Chem Rev 116:10075–10166
2. Thiagarajah JR, Jayaraman S, Naftalin RJ, Verkman AS (2001) In vivo fluorescence measurement of Na(+) concentration in the pericryptal space of mouse descending colon. Am J Physiol Cell Physiol 281:C1898–C1903
3. Gotor R, Costero AM, Gaviña P, Gil S (2014) Ratiometric double channel borondipyrromethene based chemodosimeter for the selective detection of nerve agent mimics. Dyes Pigments 108:76–83
4. Vázquez-Romero A et al (2013) Multicomponent reactions for de novo synthesis of bodipy probes: in vivo imaging of phagocytic macrophages. J Am Chem Soc 135:16018–16021
5. Ormond A, Freeman H (2013) Dye sensitizers for photodynamic therapy. Materials (Basel) 6(817–840)
6. Moreira LM et al (2008) Photodynamic therapy: Porphyrins and phthalocyanines as photosensitizers. Aust J Chem 61:741–754
7. Loudet A, Burgess K (2007) BODIPY dyes and their derivatives: syntheses and spectroscopic properties. Chem Rev 107:4891–4932
8. Wu W, Guo H, Wu W, Ji S, Zhao J (2011) Organic triplet sensitizer library derived from a single chromophore (BODIPY) with long-lived triplet excited state for triplet-triplet annihilation based upconversion. J Organomet Chem 76:7056–7064
9. Guo S, Tao R, Zhao J (2014) Photoredox catalytic organic reactions promoted with broadband visible light-absorbing Bodipy-iodo-aza-Bodipy triad photocatalyst. RSC Adv 4:36131–36139
10. Tobin JM et al (2016) BODIPY-based conjugated microporous polymers as reusable heterogeneous photosensitisers in a photochemical flow reactor. Polym Chem 7:6662–6670
11. Üçüncü M et al (2017) BODIPY-au(I): a photosensitizer for singlet oxygen generation and photodynamic therapy. Org Lett 19:2522–2525
12. DeRosa MC, Crutchley RJ (2002) Photosensitized singlet oxygen and its applications. Coord Chem Rev 233–234:351–371
13. Ghogare AA, Greer A (2016) Using singlet oxygen to synthesize natural products and drugs. Chem Rev 116:9994–10034
14. Günther, Schenck O, Ziegler K (1944) Die Synthese des Ascaridols. *Naturwissenschaften* **32**:157
15. Corsello MA, Garg NK (2015) Synthetic chemistry fuels interdisciplinary approaches to the production of artemisinin. Nat Prod Rep 32:359–366
16. World Health Organization. World Health Statistics 2017 : Monitoring health for the SDGs. World Health Organization (2017). https://doi.org/10.1017/CBO9781107415324.004
17. Nakata K, Fujishima A (2012) TiO 2 photocatalysis: design and applications. J Photochem Photobiol C: Photochem Rev 13:169–189
18. Wang X, Blechert S, Antonietti M (2012) Polymeric graphitic carbon nitride for heterogeneous Photocatalysis. ACS Catal 2:1596–1606
19. Mills A, LeHunte S (1997) An overview of semiconductor photocatalysis. J Photochem Photobiol A Chem 108:1–35
20. Plutschack MB, Pieber B, Gilmore K, Seeberger PH (2017) The Hitchhiker's guide to flow chemistry. Chem Rev 117:11796–11893
21. The Royal Swedish Academy of Sciences. The Nobel Prize in Chemistry 1984 - NobelPrize.org. *Nobel Media AB* (2019). Available at: https://www.nobelprize.org/prizes/chemistry/1984/summary/. (Accessed: 24th July 2019)
22. Palomo JM (2014) Solid-phase peptide synthesis: an overview focused on the preparation of biologically relevant peptides. RSC Adv 4:32658–32672
23. Jaradat DMM (2018) Thirteen decades of peptide synthesis: key developments in solid phase peptide synthesis and amide bond formation utilized in peptide ligation. Amino Acids 50:39–68
24. Bristow TWT et al (2014) On-line monitoring of continuous flow chemical synthesis using a portable, small footprint mass spectrometer. J Am Soc Mass Spectrom 25:1794–1802
25. Giraudeau P, Felpin FX (2018) Flow reactors integrated with in-line monitoring using benchtop NMR spectroscopy. React Chem Eng 3:399–413
26. Carter CF et al (2010) ReactIR flow cell: a new analytical tool for continuous flow chemical processing. Org Process Res Dev 14:393–404
27. Yue J, Falke FH, Schouten JC, Nijhuis TA (2013) Microreactors with integrated UV/Vis spectroscopic detection for online process analysis under segmented flow. Lab Chip 13:4855–4863
28. Schlindwein W et al (2018) In-line UV-Vis spectroscopy as a fast-working process analytical technology (PAT) during early phase product development using hot melt extrusion (HME). Pharmaceutics 10:166
29. Ribeiro SM, Serra AC, Gonsalves AMd'A (2007) Covalent immobilized porphyrins as photooxidation catalysts. Tetrahedron 63:7885–7891
30. Benaglia M, Danelli T, Fabris F, Sperandio D, Pozzi G (2002) Poly(ethylene glycol)-supported tetrahydroxyphenyl porphyrin: a convenient, recyclable catalyst for photooxidation reactions. Org Lett 4:4229–4232
31. Griesbeck AG, El-Idreesy TT, Bartoschek A (2004) Photooxygenation in polystyrene beads with covalently and non-covalently bound Tetraarylporphyrin sensitizers. Adv Synth Catal 346:245–251
32. Kitamura N, Yamada K, Ueno K, Iwata S (2006) Photodecomposition of phenol by silica-supported porphyrin derivative in polymer microchannel chips. J Photochem Photobiol A Chem 184:170–176
33. Silva M et al (2009) Immobilization of 5,10,15,20-tetrakis-(2-fluorophenyl)porphyrin into MCM-41 and NaY: routes toward photodegradation of pesticides. Pure Appl Chem 81:2025–2033
34. Han X, Bourne RA, Poliakoff M, George MW (2011) Immobilised photosensitisers for continuous flow reactions of singlet oxygen in supercritical carbon dioxide. Chem Sci 2:1059–1067
35. Grazon C, Rieger J, Charleux B, Clavier G, Méallet-Renault R (2014) Ultrabright BODIPY-tagged polystyrene nanoparticles:

study of concentration effect on Photophysical properties. J Phys Chem C 118:13945–13952
36. Wittmershaus BP, Skibicki JJ, McLafferty JB, Zhang Y-Z, Swan S (2001) Spectral properties of single BODIPY dyes in polystyrene microspheres and in solutions. J Fluoresc 11:119–128
37. Liu J, Tobin JM, Xu Z, Vilela F (2015) Facile synthesis of a conjugated microporous polymeric monolith via copper-free Sonogashira-Hagihara cross-coupling in water under aerobic conditions. Polym Chem 6:7251–7255
38. Coskun A, Deniz E, Akkaya EU (2005) Effective PET and ICT switching of boradiazaindacene emission: a unimolecular, emission-mode, molecular half-subtractor with reconfigurable logic gates. Org Lett 7:5187–5189
39. Gaspa S, Porcheddu A, De Luca L (2015) Metal-free direct oxidation of aldehydes to esters using TCCA. Org Lett 17:3666–3669
40. Guha NR et al (2018) Evaluating polymer-supported isothiourea catalysis in industrially-preferable solvents for the acylative kinetic resolution of secondary and tertiary heterocyclic alcohols in batch and flow. Green Chem 20:4537–4546
41. Bartelmess J et al (2014) Boron dipyrromethene (BODIPY) functionalized carbon nano-onions for high resolution cellular imaging. Nanoscale 6:13761–13769
42. Tobin JM et al (2017) Polymer-supported photosensitizers for oxidative organic transformations in flow and under visible light irradiation. ACS Catal 7:4602–4612
43. Shen J et al (2016) Photoactive and metal-free polyamide-based polymers for water and wastewater treatment under visible light irradiation. Appl Catal B Environ 193:226–233
44. Schweitzer C, Schmidt R (2003) Physical mechanisms of generation and deactivation of singlet oxygen. Chem Rev 103:1685–1758
45. Griesbeck AG, de Kiff A, Neudoerfl JM, Sillner S (2015) Singlet oxygen addition to cyclo-1,3-hexadienes from natural sources and from organocatalytic enal dimerization. Arkivoc 2015(101)
46. Hone CA, Kappe CO (2019) The use of molecular oxygen for liquid phase aerobic oxidations in continuous flow. Top Curr Chem 377:1–44
47. Han X, Bourne RA, Poliakoff M, George MW (2009) Strategies for cleaner oxidations using photochemically generated singlet oxygen in supercritical carbon dioxide. Green Chem 11:1787–1792
48. Gareis T, Huber C, Wolfbeis OS, Daub J (1997) Phenol/phenolate-dependent on/off switching of the luminescence of 4,4-difluoro-4-bora-3a,4a-diaza-s-indacenes. Chem Commun:1717–1718
49. Ji S et al (2015) Molecular structure-intersystem crossing relationship of heavy-atom-free bodipy triplet photosensitizers. J Organomet Chem 80:5958–5963
50. Wang L et al (2013) Regioselective 2,6-dihalogenation of BODIPYs in 1,1,1,3,3,3-hexafluoro-2-propanol and preparation of novel *meso*-alkyl polymeric BODIPY dyes. RSC Adv 3:9219

Dr. Filipe Vilela gained his expertise in polymer chemistry and organic semiconducting materials through his PhD with Prof. D.C. Sherrington FRS and post-doctoral research in the group of Prof. P.J. Skabara at the university of Strathclyde, Glasgow. He combined his expertise in these two fields to begin his independent research in heterogeneous photocatalysis as a research group leader at the Max Planck Institute of Colloids and Interfaces, Potsdam, Germany. Now an Associate Professor at Heriot-Watt University, Edinburgh, Filipe has made continuous-flow chemistry an integral part of his research to greatly enhance the photocatalytic efficiency of novel polymeric materials. In this contribution, Filipe and co-workers have established a metal-free synthesis of polymer-supported BODIPY photosensitisers in continuous-flow. They demonstrated that post-synthetic modifications of solid matrixes in flow resulted in higher coupling efficiency, accelerated purification and far less cumbersome set-up relative to the analogous batch synthesis. A unique synthetic advantage of the heterogeneous flow-synthesis was found serendipitously, which prevented an uncontrolled side-reaction identified in the synthesis of molecular analogues of the supported-photosensitiser. Generation of singlet oxygen by molecular and material photosensitisers was enhanced by a factor of 2-4 relative to batch. Reaction monitoring was achieved with an in-line 1H-NMR spectrometer and used to optimise pressure and flow-rate, which in combination with further synthetic modification to the supported BODIPY, led to an impressive 24-fold enhancement of photosensitisation efficiency relative to the initial material and conditions.